Vol. 31 • No. 42 • October 18 • 2019

www.advmat.de

ADVANCED MATERIALS

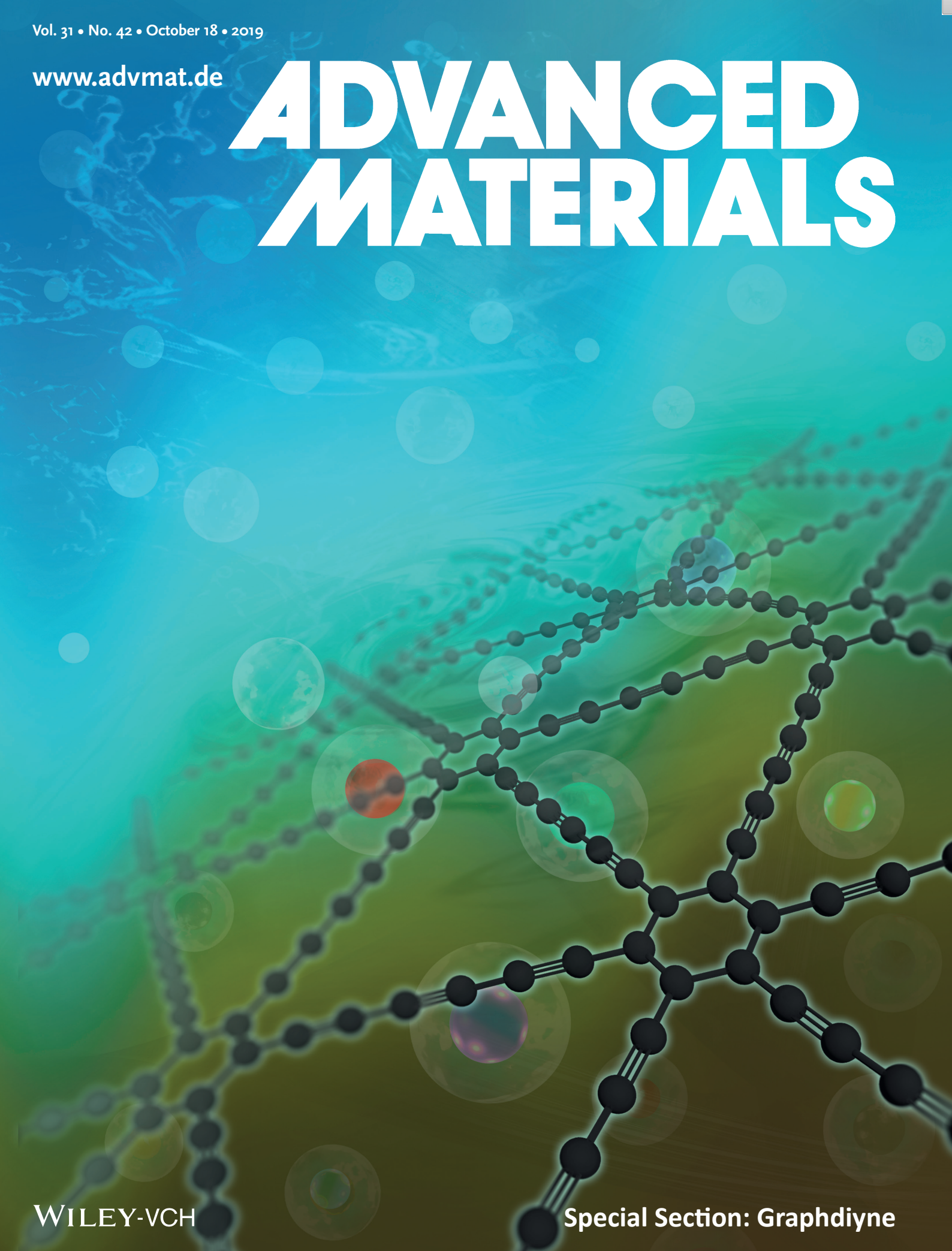

WILEY-VCH

Special Section: Graphdiyne

ADVANCED MATERIALS
www.advmat.de

Graphynes for Water Desalination and Gas Separation

Hu Qiu, Minmin Xue, Chun Shen, Zhuhua Zhang, and Wanlin Guo**

Selective transport of mass through membranes, so-called separation, is fundamental to many industrial applications, e.g., water desalination and gas separation. Graphynes, graphene analogs yet containing intrinsic uniformly distributed pores, are excellent candidates for highly permeable and selective membranes owing to their extreme thinness and high porosity. Graphynes exhibit computationally determined separation performance far beyond experimentally measured values of commercial state-of-the-art polyamide membranes; they also offer advantages over other atomically thin membranes like porous graphene in terms of controllability in pore geometry. Here, recent progress in proof-of-concept computational research into various graphynes for water desalination and gas separation is discussed, and their theoretically predicted outstanding permeability and selectivity are highlighted. Challenges associated with the future development of graphyne-based membranes are further analyzed, concentrating on controlled synthesis of graphyne, maintenance of high structural stability to withstand loading pressures, as well as the demand for accurate computational characterization of separation performance. Finally, possible directions are discussed to align future efforts in order to push graphynes and other 2D material membranes toward practical separation applications.

1. Introduction

Membranes are thin selective barriers that allow for the transport of desired species while concurrently obstructing the passage of others. Progress over recent decades in membrane technology has facilitated a variety of important industrial separation processes such as water desalination and gas purification. In particular, water desalination with reverse osmosis (RO) membranes is recognized as one of the most important routes to bridge the gap between the increasing demand for fresh water and the reduction in its availability. To date, about half of installed desalination plants worldwide rely on membrane-based RO separations due to their low energy consumption, easy operation and convenient maintenance with respect to other desalination technologies such as distillation-based thermal processes.[1,2] Current commercial membranes in RO desalination industry are dominated by thin-film composite (TFC) polyamide membranes, which consist of a thin selective layer and several underlying support layers.[3–6] The selective layer, also known as the active layer, is usually made of a dense, highly crosslinked polyamide film, with an estimated mean pore size of $<\approx 0.6$ nm and a membrane thickness between hundreds of nanometers to a few micrometers (**Figure 1**).[3] Additionally, polyamide membranes with different microscopic structures have also been developed for other separation purposes such as nanofiltration (NF). By contrast, current microfiltration (MF) and ultrafiltration (UF) membranes, widely used in pretreatment of feed seawater prior to RO processes and production of clean water from nonsaline sources, are typically created through polymer phase inversion based on other polymer materials such as poly(vinylidene fluoride) (PVDF) and polysulfone (Figure 1).[7]

In theory, an ideal membrane should enable not only the flow of desired species (e.g., water molecules in RO) as fast as possible to maximize permeance (flux), but also the complete rejection of unwanted species (e.g., salt ions in RO) to achieve high selectivity. Nevertheless, achieving such a membrane is extremely difficult, as a trade-off exists between the permeability (membrane thickness normalized flux) and selectivity, meaning that an enhancement in water permeability is usually accomplished by an even greater increment in solute permeability. The consequence of this trade-off to current TFC membrane-based RO technology is a few drawbacks such as low desalination capacity, high energy and infrastructure costs;[8–10] overcoming this trade-off is desired to further broaden RO applications, especially in less developed areas. In addition, the state-of-the-art TFC membranes maintain the same design as three decades ago, and worse yet, experienced limited improvement in membrane permeability.[3] Recent work created, by means of 3D printing, polyamide RO membranes with thickness as low as 15 nm, which exhibited comparable performance as commercial membranes but offered tunable control over the membrane thickness and roughness.[11] Thanks to the fast development of nanotechnology, these disadvantages of TFC membranes could potentially be addressed by the use of fundamentally novel membrane materials, e.g., nanoporous materials that can have well-defined pores with diameters approaching those of target species.[1,8–10,12] In the context of separation applications, these nanomaterials hold great promise as highly permeable and selective membranes, with the possibility of precise control over pore dimension and functionalization.

Dr. H. Qiu, Dr. M. Xue, C. Shen, Dr. Z. Zhang, Prof. W. Guo
State Key Laboratory of Mechanics and Control of Mechanical Structures and Key Laboratory for Intelligent Nano Materials and Devices of MoE
Institute of Nanoscience
Nanjing University of Aeronautics and Astronautics
29 Yudao Street, Nanjing 210016, China
E-mail: qiuhu@nuaa.edu.cn; wlguo@nuaa.edu.cn

DOI: 10.1002/adma.201803772

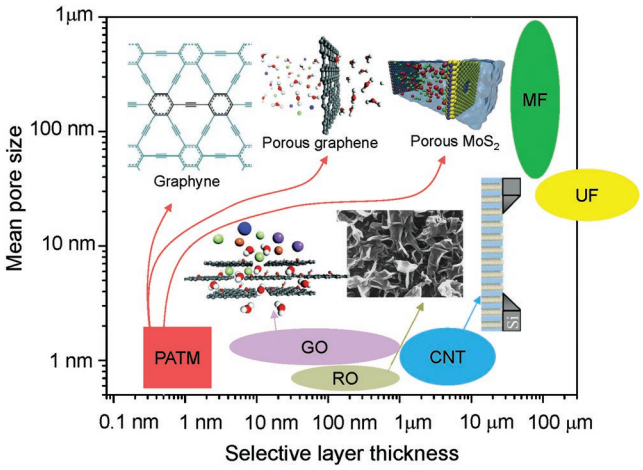

Figure 1. Mean pore size versus selective layer thickness of current state-of-the-art commercial membranes as well as nanostructured membranes. Current separation technology relies on polyamide membranes designed for various processes such as microfiltration (MF), ultrafiltration (UF), and reverse osmosis (RO). Porous atomically thin membranes (PATM) such as graphene, MoS_2, and graphyne possess a thickness of ≈1 nm (depending on the number of layers). The data for pore size and membrane thickness were recompiled from refs. [3,5] and [1,6] respectively. Note that MF and UF membranes have identifiable pores, while RO membrane is effectively nonporous and its mean pore size was estimated based on the hydrated diameters of the smallest rejected ions. Images of membranes adapted with permission from the following references: ref. [15], Copyright 2008, National Academy of Sciences (carbon nanotubes (CNT)); ref. [4], Copyright 1999, Elsevier (polyamide RO); ref. [20], Copyright 2016, Royal Society of Chemistry (graphene oxide (GO)); ref. [27], Copyright 2015, Nature Publishing Group (porous MoS_2); ref. [20], Copyright 2016, Royal Society of Chemistry (porous graphene); ref. [39], Copyright 2013, IOP Publishing (graphyne).

In contrast to polyamide membranes where molecules like H_2O diffuse slowly through a solution diffusion process, nanoporous membranes containing inherent ordered channels can permit an unexpectedly fast water flow as the molecular sieving mechanism usually governs such processes. The first series of proposed nanoporous membranes include zeolites[13] and carbon nanotubes (CNTs).[14,15] In particular, a number of simulations and experiments have shown enhanced water flow in CNTs,[14,16] due to low friction between ordered water structure and nanotube inner wall surfaces. Fornasiero et al. showed that micrometer-scale-thick membranes consisting of an array of sub-2-nm-diameter CNTs functionalized with negatively charged groups at their pore entrance rejected the permeation of >90% anions when using a 1.0×10^{-3} M $K_3Fe(CN)_6$ solution as the feed solution.[15] However, aiming to improve salt rejection, further efforts are needed to fabricate CNT membranes containing highly aligned nanotubes with sub-nanometer diameters as well as to develop and optimize pore functionalization.[17] In addition, another promising nanomaterial, graphene oxide (GO), with a thickness usually in the nanometer range (1–100 nm), has gained the attention of scientists and was also widely explored as high-performance separation membranes.[9,18–20] A schematic illustration of the mentioned membranes arranged in terms of mean pore size and membrane thickness is provided in Figure 1.

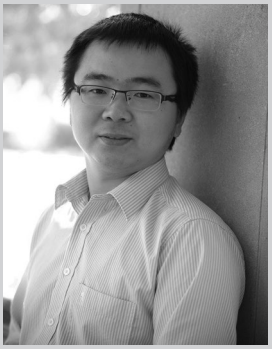

Hu Qiu received his Ph.D. degree from Nanjing University of Aeronautics and Astronautics (NUAA) in 2013. As a postdoc, he worked at the University of Illinois at Urbana-Champaign (2014–2016). In 2016, he returned to NUAA and has been an associate professor in the State Key Laboratory of Mechanics and Control for Mechanical Structures. His current research interests are the theoretical and computational understanding of nanoconfined systems.

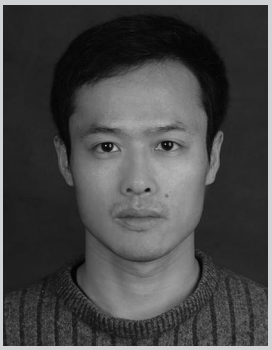

Minmin Xue received his bachelor's degree from Nanjing University of Aeronautics and Astronautics in 2011. Since then, he became a Ph.D. candidate supervised by Prof. Wanlin Guo and obtained his degree in September 2018. In 2016, he studied in the Molecular Dynamics group led by Prof. Siewert-Jan Marrink at the University of Groningen. His current research focuses on interfaces in biological and artificial nanoscale systems.

Wanlin Guo obtained his Ph.D. degree from Northwestern Polytechnical University in 1991, and in 2017 he was elected as an academician of the Chinese Academy of Science. He is a Chair Professor at Nanjing University of Aeronautics and Astronautics and the founding director of the Key Laboratory of Intelligent Nano Materials and Devices of Ministry of Education.

In the past decade, atomically thin 2D materials, such as graphene and its derivatives, are of particularly interests as new membranes for separation applications.[8–10,20,21] This is partially because their minimum possible membrane thickness may lead to significantly high permeance as the flux across a membrane scales inversely with its thickness. Graphene is a 2D carbon material with each atom arranged in a honeycomb crystal lattice, exhibiting high mechanical strength and chemical robustness.[22] A number of theoretical and computational

studies have predicted that the desalination performance of nanoporous graphene is several orders of magnitude higher than conventional polyamide RO membranes, and identified the pore size and pore chemistry being the decisive factors.[23,24] Inspired by these theoretical predictions, Surwade et al. experimentally fabricated a desalination device by placing a monolayer graphene (with dimensions of >50 μm and ≈1 nm pores) on a 5 μm diameter aperture, and measured a nearly 100% salt rejection rate as well as a high water permeability.[25] The driving pressure, induced by gravity of salt solutions on top of the porous graphene, was estimated to be ≈17 kPa (which is much lower than typical operating pressures used in industrial desalination processes, at 5.5–6.9 MPa).[25] Aside from graphene, other atomically thin materials such as MoS_2[26,27] were also explored as alternatives to current RO membranes, again exhibiting remarkable separation performance. However, to fulfill such separation applications, nanopores have to be created on these atomically thin membranes by various methods such as electron beam, ion beam drilling and chemical etching.[20,21,28] Despite plenty of efforts made to this end, controlled formation of nanopores with uniform shape and size on a graphene sheet remains extremely challenging,[9,20] which requires further breakthroughs in experimental technologies relating to pore creation or search for other 2D materials with intrinsic porosity.

Graphyne is a relatively new family of carbon allotropes, also with the thickness of merely one atom. However, unlike graphene that is formed entirely by a sp^2-hybridized carbon network, graphyne consists of an arranged structure of benzene and alkyne units containing both sp- and sp^2-hybridized carbon atoms (**Figure 2**). The most striking feature that distinguishes graphyne from other nanoporous materials is the containing of intrinsic uniform well-defined pores; these pores are usually formed by acetylenic linkages of various lengths connecting the alkyne or benzene units of graphynes. Meanwhile, the pore shape and dimension vary due to different arrangement of the acetylene and phenyl groups, as well as the number of acetylenic linkages, giving rise to a large population of members existing in the graphyne family. These structural characteristics render graphynes as one of the most promising candidates for next-generation separation membranes. In addition, breakthroughs in experimental fabrication of a graphyne structure (i.e., graphdiyne, described in Section 2) on copper surfaces made by Li and co-workers[29,30] largely stimulated subsequent efforts to exploit graphynes' various applications, including the membrane-based separations, the topic of this article.

A number of reviews have been published in the past years focusing on the development of nanomaterials as nanoporous separation membranes,[9,10,12,19,21,28,31,32] but none of them concentrating solely on graphynes. On the other hand, there are also a few excellent reviews highlighting computational characterization of physical properties, chemical synthesis of graphynes as well as their potential applications.[30,33,34] Here, we intended to provide a timely overview of important progress solely on the utilization of graphynes as high-performance membranes, aiming to push graphynes toward practical separation applications to revolutionize membrane-based water desalination and gas separation technologies. Particularly, a careful literature survey was made, focusing on theoretical progress and experimental challenges related to the design of graphyne-based separation membranes. Herein, Section 2 briefly describes the basic units of graphynes, and highlights typical graphyne structures with features potentially suitable for separation applications. Section 3 covers most of recent progress in theoretical investigations of graphynes for applications in water desalination and purification as well as gas separation. Finally, we will close by Sections 4 and 5 with a discussion on remaining challenges, future prospective and opportunities related to further development of graphyne-based membranes, emphasizing on the previous efforts made already by experimentalists and needed in future to advance graphyne toward practical applications.

2. Basic Structures of Graphynes

As one of the most abundant elements found in nature, carbon forms diverse allotropes with carbon atoms in various hybridization states including sp, sp^2, and sp^3.[35] The conventional well-known carbon allotropes are naturally found diamond and graphite, consisting of sp^3- and sp^2-hybridized carbon atoms, respectively. Successive discovery of 0D fullerenes,[36] 1D carbon nanotubes,[37] and 2D graphene,[38] all comprising solely sp^2-hybridized carbon atoms, largely expanded the family of carbon allotropes. Resembling graphene, graphyne is another one-atom-thick carbon allotrope, yet consisting of both sp and sp^2 carbon atoms. From a geometric point of view, graphynes can be simply regarded as being constructed by substituting some =C=C= bonds in graphene with a few uniformly distributed acetylenic linkages −C≡C−. Graphyne has received substantial interests in diverse applications including membrane separations,[39–43] transistors,[44] field emission devices,[45] battery electrode materials,[46] catalysts[47] and sensors,[48] inspired by its impressive structural, electronic, and mechanical properties.

The structures of typical graphynes are illustrated in Figure 2. In general, graphynes can be constructed by the combination of two basic structural units: benzene rings and acetylenic linkages, as provided in the smallest green sector region of Figure 2. Theoretically, it is reasonable to form a great number of allotropes of graphynes via different combinations. The simplest combination of these two units yields a structure family of graphyne known as graphyne-*n* (or graph-*n*-yne), with *n* being the number of acetylenic linkages (such unit acetylenic linkages are highlighted in red). In the case of $n = 1$, for example, a single acetylenic linkage (−C≡C−) connects two adjacent benzene rings, leading to a structure termed as γ-graphyne. In particular, increasing the number of acetylenic linkages to $n = 2$ gives rise to another carbon allotrope with again a designated name, graphdiyne, which attracts majority of attention in the graphyne family, mainly because graphdiyne is the only graphyne that has been successfully synthesized.[29,30] Likewise, further addition of the alkyne units to $n = 3$ leads to graphyne-3, a promising candidate for water desalination and purification which we will discuss later. Following this strategy, the size of nanopores in this carbon network containing acetylenic linkages can be readily adjusted by choosing a different *n*, which is undoubtedly attractive for separation applications relying on steric resistance mechanism.

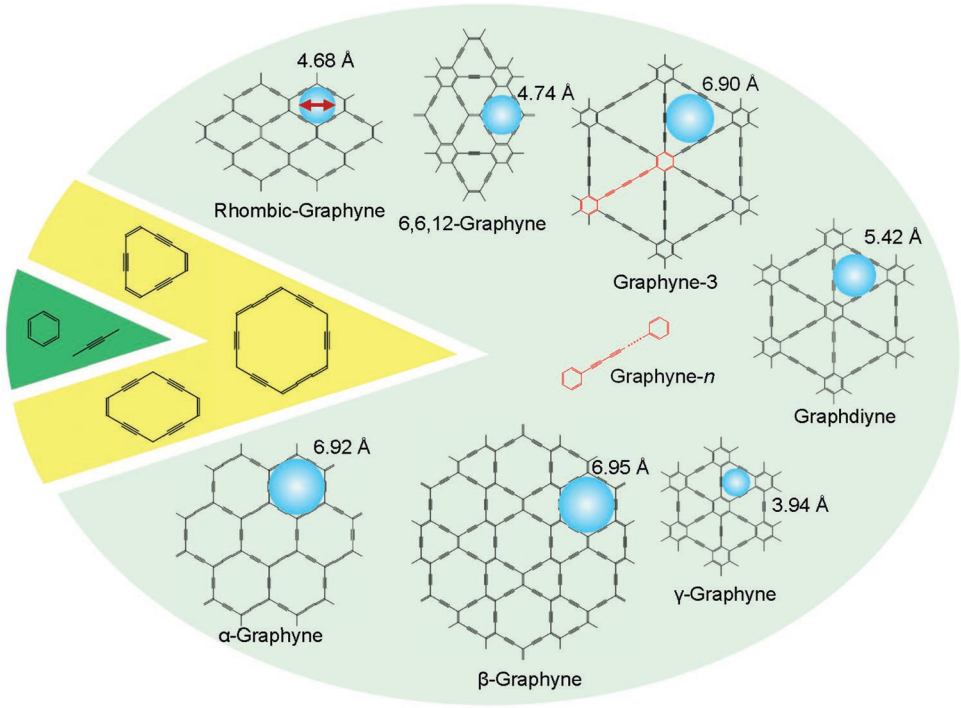

Figure 2. Various structures of graphyne. The blue hollow spheres indicate the inscribed circles of nanopores in different graphynes, with diameters labeled aside. The green and yellow sector-shaped regions highlight typical building blocks of graphynes.

The yellow intermediate sector region in Figure 2 highlights three larger rings of different size and shape encountered in most graphyne structures; these rings could be regarded as formed by replacing three, four or six =C=C= bonds in a benzene ring with the acetylenic linkages −C≡C−. These three large rings, along with the benzene ring itself, can constitute all the remaining graphynes shown in Figure 2, namely α-graphyne, β-graphyne, 6,6,12-graphyne and rhombic-graphyne.

The unique feature that renders graphyne as a promising membrane material is its intrinsic nanopores. We note that all nanopores in graphyne possess an inscribed circle (shown in blue spheres) that is defined by the linear chain containing acetylenic linkages; the size of the inscribed circle varies in different graphynes. A straightforward comparison of the pore size with the sizes of target molecules and ions (**Table 1**) could lead to a rough evaluation of the suitability of graphynes for target separation applications, by assuming that the steric resistance dominates the separation (i.e., via molecular sieving). Nevertheless, to validate such estimation, comprehensive investigations are needed, which we now discuss.

Table 1. Size of typical molecules and ions involved in graphyne-based separation processes.

Species [a]	Size [Å]
Molecules (kinetic diameter)	He (2.6), H_2 (2.89), CO_2 (3.3), CO (3.76), CH_4 (3.8), N_2 (3.64), O_2 (3.46), C_2H_6O (4.53), H_2O (2.65)
Ion (diameter of hydrated ions)	Na^+ (7.16), Cl^- (6.64), K^+ (6.62), Mg^{2+} (8.56), Ca^{2+} (8.24)

[a] Recompiled data.[10]

3. Operation as Separation Membranes

Typically, a sheet of perfect graphene is impermeable to molecules as small as helium,[49] and therefore nanometer-sized pores have to be fabricated in graphene prior to any separation applications, during which the precise control over pore size and chemical functionalization is technically challenging. In this context, the intrinsic nanopores in graphynes, with uniformly distributed shape and dimension, have attracted much attention in the community of membrane science and engineering.

We fulfilled a thorough literature survey and noted that all the existing graphyne-based separation studies, as summarized in **Table 2**, are from a theoretical viewpoint and based on computations. Computation has proved itself an useful tool in material research in predicting material structures, understanding molecular-scale interactions, as well as guiding relevant experimental researches.[8,24] Prevailing computational modeling approaches include quantum mechanics (QM) calculations, molecular dynamics (MD) simulations as well as their combination, QM/MD simulations. At the QM level, interactions at electronic resolution are described by solving the Schrödinger wave equation either directly or by employing functionals with approximations at various levels (e.g., density functional theory (DFT)). In QM simulations, nuclei and electrons are explicitly considered, therefore the properties of materials can be computed with accurate quantum effects. QM methods are useful in reliably resolving the energy barrier of individual molecules permeating through graphyne pores. However, due to their expensive computational cost, very small systems containing hundreds of atoms are usually considered.

Table 2. Summary of computational studies on graphyne-based separations.

	Graphyne types	Desired species	Rejected species	Methods	Year	Ref.
Liquid separation	α-/β-Graphyne, graphdiyne,[a] graphyne-3/-4	H_2O	Na^+, K^+, Cl^-, Mg^{2+}, Ca^{2+}	MD	2013	[39]
	Graphyne-3/-4/-5/-6	H_2O	$CuSO_4$, C_6H_6, CCl_4, NaCl	MD	2013	[40]
	γ-Graphyne,[a] graphdiyne[a], graphyne-3/-4/-5/-6	H_2O	Na^+, Cl^-	MD, QM/MD	2013	[41]
	Graphyne-3/-4/-5	H_2O	Na^+, Cl^-	MD	2014	[52]
	Graphyne-3/-4/-5/-6	H_2O	Na^+, Cl^-	MD	2015	[56]
	Graphyne-3/-4/-5	CH_3CH_2OH	H_2O	MD	2016	[58]
	Pristine/charged graphyne-3/-4/-5	H_2O	Na^+, Cl^-	MD	2017	[54]
	Graphyne-3/-4/-5	CH_3CH_2OH	H_2O	QM, MD	2017	[59]
	Bilayer graphyne-3/-4	H_2O	Na^+, Cl^-	MD	2018	[95]
	Pristine/hydrogenated α-graphyne, graphdiyne, graphyne-3/-4	H_2O	Na^+, Cl^-	MD	2018	[55]
	Graphyne-3/-4/-5	CH_3CH_2OH	H_2O	MD	2018	[60]
Gas separation	Graphdiyne	H_2	CO, CH_4	QM	2011	[42]
	Graphdiyne	H_2	CO, CH_4	MD	2012	[43]
	γ-Graphyne,[a] rhombic-graphyne, graphdiyne	H_2	CO, N_2, CH_4	QM	2012	[70]
	Graphdiyne	H_2	CO, N_2, CH_4	MD	2012	[71]
	Graphdiyne	He, Ne	CH_4	QM	2014	[72]
	Hydrogenated γ[a]/α-graphyne	H_2	N_2, CH_4	MD	2015	[78]
	Nitrogen-doped graphdiyne	H_2	CO, CH_4	QM	2015	[75]
	Charged graphdiyne	H_2	CO, CH_4	QM	2015	[77]
	Multilayer graphyne-3	CO_2	H_2, N_2, H_2O	QM	2016	[94]
	Graphdiyne	O2	Cl_2, HCl, HCN, CNCl, SO_2, H_2S, NH_3, CH_2O	QM	2016	[74]
	Dumbbell-shaped γ-graphyne	H_2	H_2O, CO_2, N_2, CO, CH_4	QM, MD	2017	[79]
	Nitrogen-doped graphdiyne	He	H_2O, Ar, CO_2, N_2, CH_4, CO	QM, MD	2017	[76]
	Hydrogen[a]-/fluorine-/oxygen-modified graphdiyne	CO_2, N_2	CH_4	QM, MD	2017	[80]
	Oxygen-modified graphdiyne	CO_2	N_2	QM,MD	2017	[80]
	Multilayer graphyne-3	CO_2	N_2	QM, MD	2018	[73]

[a]Graphynes that were proven unsuitable for intended separation.

Compared to the QM method, classic MD simulations are computationally cheaper, allowing for direct observation of kinetic processes of much larger systems (e.g., $\approx 10^7$ atoms) over physically meaningful timescale (e.g., ≈ 1 μs). As the first step of a typical MD simulation, a model system is created by assigning each atom a given position and partial charge. By solving the Newton's equations of motion, a trajectory illustrating the time evolution of the system could be obtained. However, owing to the use of empirical force field, where interactions are described with simple potential functions, this method operates at an atomistic level and ignores chemical interactions involving electronic degrees of freedom. In MD simulations of graphyne-based separations, the model system usually consists of two gas or water reservoirs separated by a graphyne membrane. Driven by pressure gradients, the passage of individual molecules across the membrane could be monitored and analyzed.

QM/MD, the combination of QM and MD, could model time-dependent behaviors where the empirical potential functions are not sufficient to accurately describe the physics. The movement of each atom is again determined by Newton's equations of motion, while the interatomic forces are calculated with the QM methods such as ab initio and DFT, instead of the empirical potentials.

3.1. Water Desalination and Purification

3.1.1. Enhanced Permeability and/or Selectivity

Permeability and selectivity are the two important parameters to characterize the performance of a membrane material for water desalination and purification. The high permeance of pure water through a monolayer graphyne-3 was validated by MD simulations, a powerful tool to understand behaviors in nanoscale systems.[50] The fast water flow is closely related to the formation of a short single file hydrogen-bonded water chain across the graphyne-3 pore,[51] which reduces the free energy barrier at the pore entrance. On the other hand, the selectivity of graphynes has also been evaluated by MD simulations of typical RO processes.[39–41,52] **Figure 3**A depicts the schematic illustration of a spiral wound membrane module

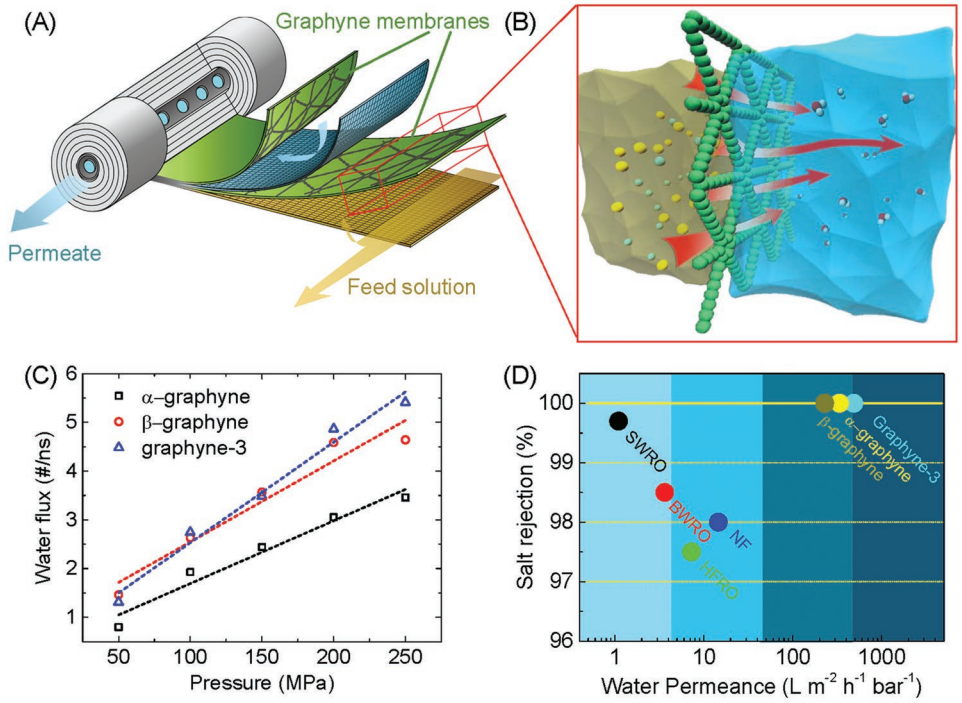

Figure 3. Graphyne-based water desalination. A) Schematic diagram of a spiral-wound RO membrane module consisting of several functional layers such as feed (olive-green meshes) and permeate (cyan meshes) spacers, as well as a selective layer using graphyne (green). In a typical RO process, water permeates through the graphyne driven by pressure gradients when salts are rejected. B) Magnified view of the RO process based on a monolayer graphyne, which is the typical set up of systems adopted in MD simulations. C) Water flux per nanopore across α-graphyne, β-graphyne and graphyne-3 as a function of external pressures. D) Performance comparison between graphynes and conventional commercial RO membranes, such as polymeric seawater RO (SWRO), brackish water RO (BWRO), high-flux RO (HFRO), and nanofiltration (NF). B–D) Adapted with permission.[39] Copyright 2013, IOP Publishing.

widely used in current commercial RO desalination techniques. It consists of a thin selective layer (here, graphyne) being sandwiched with several other functional layers. The chemically inert surface, excellent mechanical strength, well-defined open pore as well as high porosity make graphyne an ideal material for such selective layer.[30,53] With this in mind, one could then build an MD simulation system (see, for example, Figure 3B), which consists of a monolayer sheet of graphyne separating a reservoir into two compartments, and test the suitability of various graphynes as the selective layer. In order to induce the flow of water across this layer, an external pressure gradient is usually applied between the two compartments.

In 2013, our group systematically assessed the desalination performance of five different graphynes including α-graphyne, β-graphyne, graphdiyne, graphyne-3, and graphyne-4 through MD simulations.[39] In general, a linear relationship is established, regardless of the graphyne type, between the water flux and external pressure (Figure 3C). For illustrative purposes, the theoretical performance of the studied ideal graphyne membranes is displayed in Figure 3D, with the experimental performance of commercial RO membranes shown as a reference. Three of the five graphynes, including α-graphyne, β-graphyne, and graphyne-3, all exhibit water permeance about two orders of magnitude higher than experimentally observed permeance for commercial RO membranes. In particular, graphyne-3 yields the highest permeance among the three graphynes. This is because graphyne-3 possesses a triangular pore with an effective pore area of ≈15.6 Å^2, larger than those of α-graphyne and β-graphyne both containing hexagonal pores of about ≈11 Å^2. It is noteworthy that β-graphyne has a relatively low porosity, which may also account for its low permeance. Another striking feature is the observation of salt rejection at 100% in most considered graphynes (Figure 3D). In addition, our results also revealed that the remaining two graphynes are likely not ideal candidates for desalination applications, as graphdiyne is impermeable to both water and ions and graphyne-4 exhibits incomplete salt rejection.[39]

Not limited to the aforementioned work, graphyne-3 was proved to be the most popular candidate in a number of simulation reports on graphyne-based desalination, and the reported water permeance in the literature falls in a narrow range (i.e., 1221,[52] 1112,[40] 563,[54] 488[39] L m^{-2} h^{-1} bar^{-1}). The slight controversy of water permeance could be attributed to the difference in simulation setup (vacuum or water reservoir at the permeate side) and/or strategy used to induce the external pressure (using a rigid piston or applying forces directly on selected water molecules). Another inconsistency lies in the salt rejection of graphyne-4. Specifically, Zhu et al. argued that a complete ion rejection (namely, 100%) could also be achieved for graphyne-4,[41] while other studies did not support this observation.[39,52,55] This inconsistency may result from the use of different force field parameters and initial structures of graphynes. Whether or not, the much higher water throughput of graphyne-4 compensates for its possible shortage in salt rejection, and therefore it may act as a membrane material tailored

to other separation applications such as nanofiltration. Not limited to RO processes, graphyne-3 was also suggested to be suitable as a membrane in forward osmosis, which exhibited a water flux of 39.15 L cm^{-2} h^{-1}, several orders of magnitude higher than conventional osmotic membranes.[56]

Interestingly, a first-principles study[57] predicted that graphdiyne can also permit the permeation of water molecules, in sharp contrast to MD studies where graphdiyne was shown to be impermeable to water.[39] Specifically, the energy barrier that a water molecule at the pore entry encounters could be readily overcome by the formation of a hydrogen bond with another water molecule on the other side of the membrane, facilitating the water passage through the pore.[57] If validated, this argument should be of significance in the area of graphyne-based desalination, as graphdiyne is the sole graphyne that has been experimentally prepared.

Apart from salt rejection, graphynes can also sieve small organic molecules from water either by size effect or chemical affinity. For graphyne-3 with a small pore size, the passage of organic molecules like CCl_4, C_6H_6, and CH_3CH_2OH are blocked under moderate pressures simply due to their relatively larger molecular diameters.[40,58–60] When the pore size increases, the organic molecules will preferentially clog into the pore area due to their stronger interfacial affinity with the hydrophobic membrane compared to water.[60] Although the permeability ratio (i.e., selectivity) of graphyne-*n* (3, 4, and 5) membranes for ethanol-water mixture is relatively low, their theoretically determined permeance is higher than those measured experimentally for commercial ethanol-permselective membranes.[60]

The performance of graphyne-based water desalination can be modulated by charge injections or chemical modifications. It was found that a charged graphyne-4 membrane tended to induce a stable water flux by reducing the inverse flow of water molecules.[54] In particular, negatively charged graphyne-4 membranes exhibit a higher permeance than positively charged membranes due to different binding affinities with counterions in the solution (i.e., ions with the opposite charge sign as the membrane), an effect believed to slow down water permeation. With the help of hydrogenation, a recent study suggested that the salt rejection rate of graphyne-3 could be improved, though with a lower water permeance (**Figure 4**).[55] Furthermore, it is interesting to note that the hydrogenated graphyne-4 pores could selectively permeate negatively charged ions such as Cl^- while blocking positively charged ions like Na^+ and K^+; a completely opposite trend was seen in oxygenated graphyne-4.

By examining the development path for membrane technologies, one should note that energy savings have been achieved through the development of TFC polyamide membranes, resulting from improved water permeability and selectivity.[61] Nevertheless, further enhancement in water permeability far beyond current TFC membranes, for example, those exhibited by graphyne-based membranes, may not be directly translated into further energy savings. Two factors can account for this argument. First, the concentration polarization at membrane

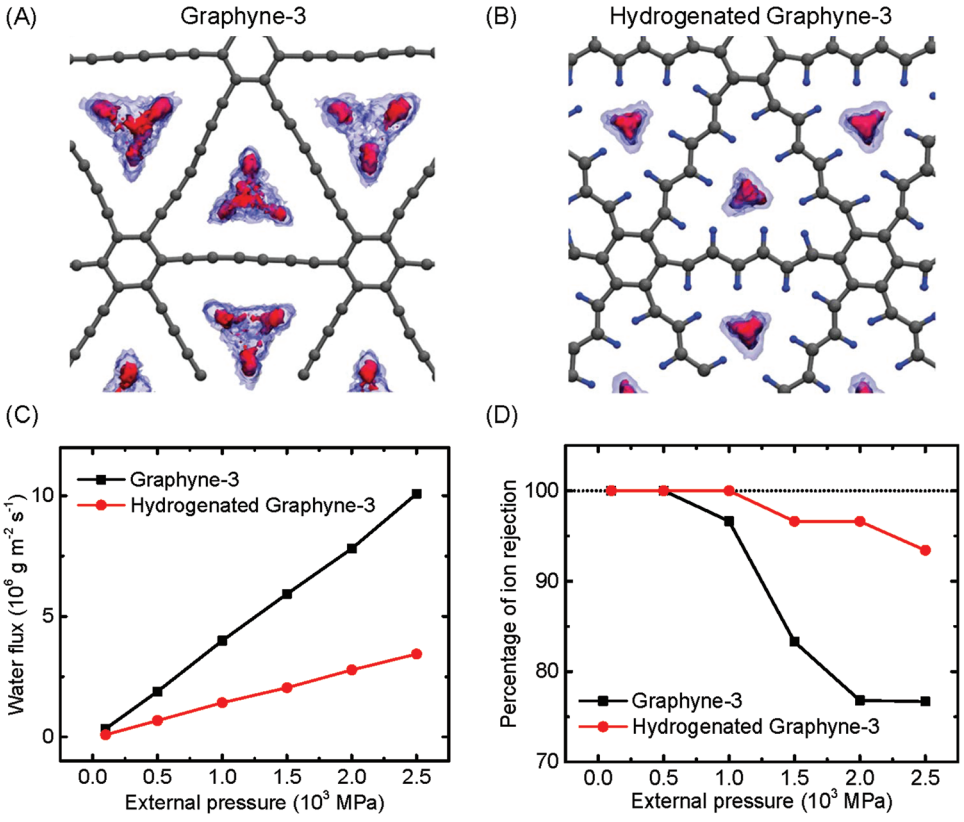

Figure 4. Modulation of desalination performance with pore functionalization in graphynes. A,B) Probability density maps of oxygen (red) and hydrogen (blue) of permeating water molecules in pristine (A) and hydrogenated graphyne-3 (B) membranes. C,D) Water flux (C) and salt rejection (D) versus applied pressure for pristine and hydrogenated graphyne-3 membranes. Reproduced with permission.[55] Copyright 2018, Royal Society of Chemistry.

surfaces limits further increase in water flux.[61] Second, the energy consumption to overcome osmotic pressure gradients is unavoidable, and has been reduced significantly due to the advent of TFC membranes.[61,62] Recent module-scale modeling results indicated that, increasing water permeability above currently achieved levels in state-of-the-art TFC membranes would lead to minor (<0.06 kWh m^{-3}) energy savings.[61] However, the high permeability of graphyne and other porous nanomaterials may help reduce the spatial footprint of high-throughput desalination plants or find applications in space-constrained desalination scenarios, as their enhanced water permeability could in principle reduce the number of pressure vessels.

3.1.2. Liquid Separation Mechanism of Graphynes

The selective transport of mass through graphynes can generally be attributed to steric resistance imposed by the pores, as the molecular sizes are usually comparable to those of typical graphyne pores. In this regard, a typical graphyne-based liquid separation is governed by the molecular sieving mechanism where undesired species (e.g., hydrated ions) are blocked or inhibited due to unfavorable size effect or chemical affinity. **Figure 5**A shows the potential mean force free energies calculated for water molecules and different ions passing through the hexagonal pore of α-graphyne.[39] It can be found that water molecules could pass through the pore almost unimpededly, indicated by the presence of an energy barrier less than ≈2 kcal mol^{-1}. For monovalent ions, a larger energy barrier of about ≈10 kcal mol^{-1} has to be overcome, making the penetration of ions infeasible. The much larger energy barrier for ions than water is associated with the presence of hydration shells around ions resulting in larger molecular sizes (with respect to bare ions).[39] In order to enter the graphyne pores, some water molecules in the first hydration shell have to be peeled off, which makes the passage of ions energetically unfavorable. Consistent with such argument, a higher energy barrier was found for divalent cations due to the much stronger hydration of these ions (Figure 5A, inset). For graphyne-*n* membranes with increased pore area (e.g., graphyne-4), fewer water molecules have to be peeled off from the ion hydration shells in order to enter the pore, leading to a reduced energy barrier of ion permeation and in turn, a lower salt rejection rate. Furthermore, the single concentration area in the in-plane water density distribution plot confirmed that water molecules align themselves in a single-file chain when permeating through nanopores in α-graphyne, β-graphyne, and graphyne-3,[39] while multiple water chains were seen in graphyne-4 pores (Figure 5B). The presence of these multiple chains should be tightly correlated with the higher permeance observed for the graphyne-4 membrane.

Another selectivity mechanism, the so-called Donnan exclusion, arises and sometimes becomes dominant when charges are introduced into the pore edges or surfaces of membranes.[3,8,9] Due to electrostatic interactions between ions and a charged membrane, the concentrations of co-ions (ions having the same charge sign as the pore charge) and counterions (ions having the opposite charge sign as the pore charge) deviate significantly from those in solutions; the membrane becomes enriched with counterions but depleted of co-ions. As a result, a Donna potential is established at the membrane–solution interface, which tends to hinder the permeation of co-ions. The Donnan exclusion principle has been proved applicable in accounting for the ion selection in charge-modified porous graphene with large nanopores[63] as well as in functionalized sub-2-nm carbon nanotube pores.[15] Likewise, in graphyne membranes, the imposed charges on pore edges could modulate the molecular transport across graphynes due to the Donnan exclusion mechanism, resulting in altered permeability or selectivity.[54,55]

3.2. Gas Separation

A typical gas separation process requires, analogous to the RO desalination process, fast permeation of desired gas species through a membrane while other gas species are rejected. A notable example of such process is the production of highly purified hydrogen with CO_2 being separated out from syngas. In industrial applications, separation membranes are often packaged into hollow fiber modules, as shown in **Figure 6**A.

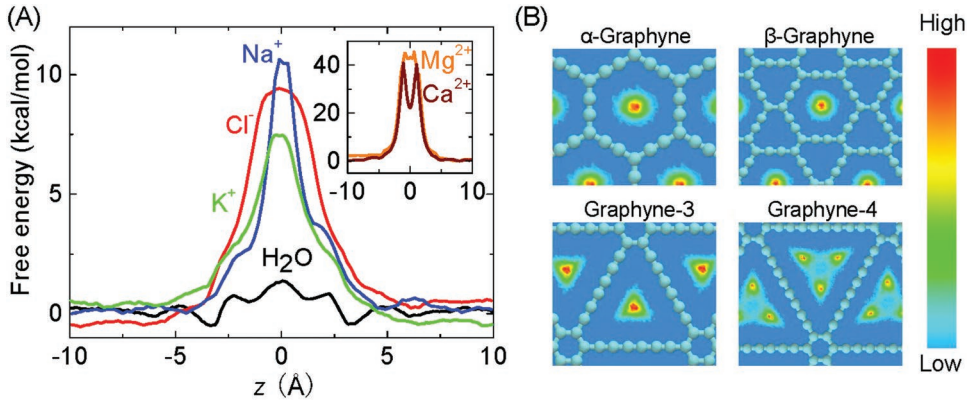

Figure 5. Transport mechanism of graphyne desalination membranes. A) Free energies for water and ions across a α-graphyne monolayer. B) Water oxygen density maps inside different graphyne pores during the separation process. A single-water water chain usually presents in α-graphyne, β-graphyne and graphyne-3 with small nanopores, while in larger graphene-4 nanopores, about three water chains exist. Reproduced with permission.[39] Copyright 2013, IOP Publishing.

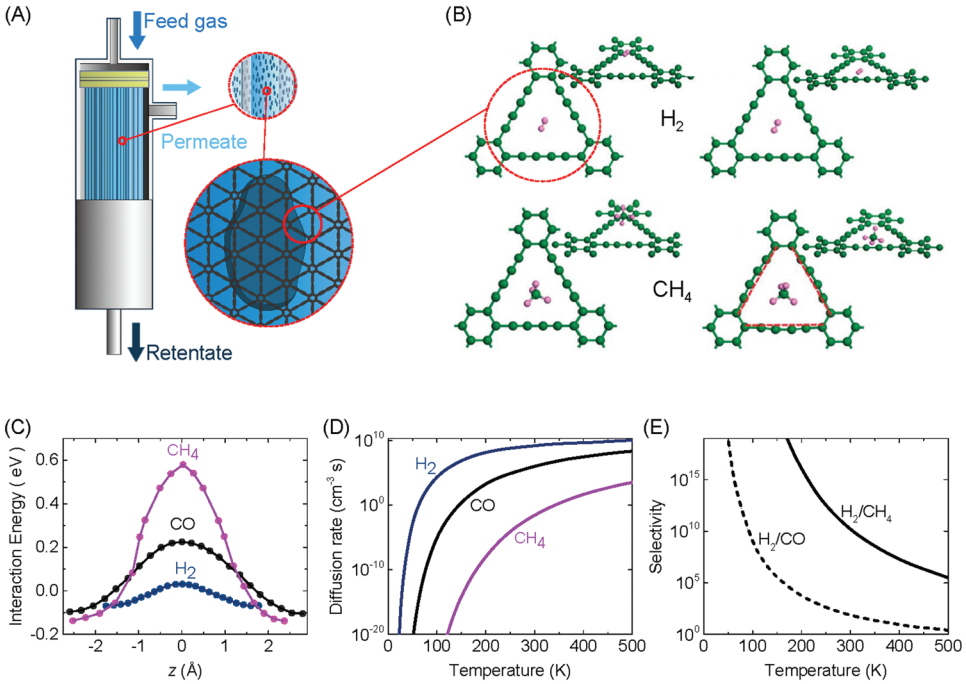

Figure 6. Graphyne-based gas separation. A) Schematic illustration of a graphyne-based membrane module for gas separation. A layer of graphyne is placed on the porous wall surfaces of hollow fibers. B) DFT-optimized configurations of H_2 (top panels) and CH_4 (bottom panels) adsorbed above (left panels) and inside the pore interior (right panels) of graphdiyne. Shown in the inset of each panel is the side view of the given configuration. C) Minimum interaction energy of H_2, CO_2 and CH_4 passing through graphdiyne. D,E) Estimated permeation rate (D) and selectivity (E) for different gases through graphdiyne at various temperatures estimated by a transition state approach. B–E) Adapted with permission.[42] Copyright 2011, Royal Society of Chemistry.

The hollow fiber usually possesses a porous wall, covered by a selective skin layer on the surface to permit fast permeation of certain gases. Driven by a pressure gradient, the feed gas is pushed into the hollow fibers, and the target gas permeates through the selective layer as the permeate stream while other gas flows inside the fiber and exits through the retentate end of the module, giving rise to the desired gas separation.

3.2.1. The Case of Graphene

Graphene-like atomically thin sheets represent as the "ultimate" membrane for alternatives to such selective layers, because their single-atom thickness could in principle lead to a negligible mass transport resistance, and in turn, a high permeance of desired gases, in the context that the permeance scales inversely proportionally to the membrane thickness. In 2009, Jiang et al. predicted through DFT calculations a high selectivity ratio on the order of 10^8 for H_2 over CH_4 and concurrently a high H_2 permeance for a nitrogen-functionalized graphene nanopore.[64] The selectivity could be further increased to the order of 10^{23} by switching the functionalization from nitrogen to hydrogen.[64] Likewise, the separation and associated energy barriers of different gases such as He,[65] N_2,[66] H_2O, CH_4, CO, CO_2, and O_2,[67] through porous graphene have also been predicted by theoretical approaches. It is encouraging that an experimental work has shown the selective gas transport through graphene nanopores fabricated by ultraviolet-induced oxidative etching.[68] Another popular method for pore creation is the focused ion beam (FIB). Nevertheless, the diameters of the FIB-drilled pores vary in a relatively broad range between 10 nm and 1 μm,[69] highlighting the demand for breakthroughs in nanomanufacturing technologies or the utilization of other atomically thin nanomaterials with intrinsic porosity, such as graphynes.

3.2.2. Graphynes as Gas Sieves

In 2011, Jiao et al. reported the first dispersion corrected DFT study on gas transport through the triangular pores in a graphdiyne sheet, as shown in Figure 6B–D.[42] An energy barrier for H_2 as low as 0.1 eV was predicted, which promises a 10^4 times faster H_2 permeation than porous graphene. On the other hand, however, the energy barriers for CH_4 and CO permeation are 0.72 and 0.33 eV, respectively, much higher than that for H_2. Subsequently, Jiao et al. employed the transition state theory to estimate the diffusion rate (Figure 6D) and selectivity (Figure 6E) of these gas molecules at various temperatures.[42] For instance, the selectivity of H_2 to CH_4 at room temperature was estimated to be 10^{10}, which is much higher than experimental values for conventional silica and carbon membranes usually on the order of 10–10^3.[42] Similarly, Zhang et al. carried out DFT calculations on the selective transport of H_2 over other gases including CO, N_2, and CH_4, through again graphdiyne, as well as γ-graphyne and rhombic-graphyne.[70] They revealed the dependence of the separation performance on the pore size. In particular, their results suggested that γ-graphyne's pore

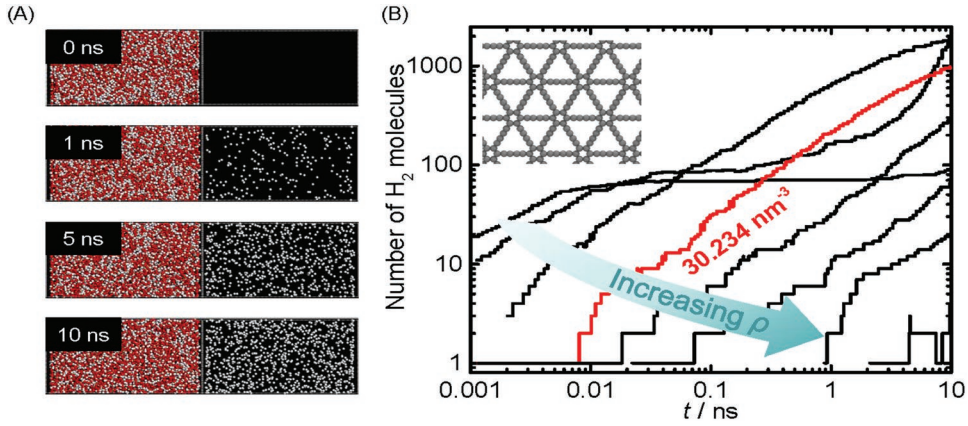

Figure 7. MD simulation of gas separation with graphdiyne. A) MD snapshots illustrating successive permeation of H_2 (white spheres) through a graphdiyne membrane, while O_2 (red spheres) permeation is always blocked. Initially, an equimolar binary mixture of H_2/O_2, having a number density $\rho = 30.234$ nm^{-3}, was placed in the left reservoir. B) The time evolution of the number of permeated H_2 molecules for H_2/O_2 mixtures at different initial ρ. The red curve corresponds to the simulation shown in (A). The inset shows the graphidyne structure. Reproduced with permission.[71] Copyright 2012, Chinese Physical Society.

was too small to allow for the permeation of any gas species including H_2, while graphdiyne and rhombic-graphyne with larger pores were identified as ideal candidates for H_2 permeation. However, the selectivity of rhombic-graphyne was better than graphdiyne, as the latter did not satisfactorily hinder the permeation of small CO and N_2 molecules. Almost simultaneously, two independent groups reported MD studies of gas transport (mainly H_2) through graphdiyne nanopores, and both predicted a high flux of H_2 while other gases like O_2, CO, and CH_4 were mostly blocked even under high pressure gradients (**Figure 7**).[43,71] In particular, the energy barrier required for H_2 molecules to pass through graphdiyne was determined to be 0.11 eV,[43] in excellent agreement with that obtained with DFT at 0.1 eV.[42] Aside from the H_2 purification, the capability of graphdiyne to separate other gas mixtures such as He and Ne over CH_4,[72] CO_2 over N_2,[73] and O_2 over harmful gases like Cl_2, HCl and NH_3[74] was also validated by theoretical approaches (listed in Table 2).

Although above progress has established exceptionally high separation performance of graphynes, a few groups reported strategies for its further improvement. Typical approaches including pore functionalization by nitrogen doping[75,76] and positive charge injection[77] have been used to reduce the barrier for H_2 or He permeation and increase that for CH_4 or CO and so on, aiming to promote permeability and/or selectivity in gas separations. These efforts therefore lead to promising strategies to somehow overcome the trade-off between membrane permeability and selectivity in the context of H_2 purification with graphdiyne. For example, Alaghemandi found in an MD study an enhanced H_2 permeance and full rejection of CH_4 in hydrogenated α-graphyne, which, in its pristine form, is likely unsuitable for such separation purpose.[78] Additionally, a combined DFT-MD study reported the excellent H_2 separation capability of a derived structure of γ-graphyne (so-called dumbbell-shaped γ-graphyne which is impermeable to H_2 in its original form), constructed by substituting one-third acetylenic linkages with nitrogen or hydrogen atoms.[79] Meanwhile, by using a similar structural architecture but derived from graphdiyne, scientists obtained a membrane that can separate gases not limited to H_2, such as CO_2 and N_2 over CH_4, when a chain of acetylenic linkages was substituted by fluorine or oxygen atoms.[80]

3.2.3. Gas Sieving Mechanism of Graphynes

In dense polymeric membranes without defined pores, the transport of gases is usually described by a solution-diffusion mechanism, where gas species are first dissolved on the membrane and then the selectivity arises from the difference in the amount of species diffusing through the membranes.[7] Other mechanisms such as Knudsen diffusion and Poiseuille flow can also govern the gas transport and separation in the case of very large pores. Specifically, the Poiseuille flow takes place in much larger membrane pores (e.g., >200 nm) with respect to the mean free path of gas molecules. In nanopores relatively smaller than the gas mean free path yet larger than molecular size (e.g., between 2 and 50 nm and at pressures under 10 bar),[7,10,81] the gas flow is dominated by the Knudsen diffusion. When the pore size falls between 50 and 200 nm (estimated at room temperature and atmospheric pressure),[81] there exists a Knudsen–Poiseuille transition region where both flow mechanisms affect gas transport. Through both mechanisms, the separation of a gas mixture could be achieved from the difference in the permeation rates of different gases. In contrast, we note that the diameters of graphyne nanopores are usually comparable to the size of target gas molecules, and thereforethe size sieving effect, a classical molecular sieving mechanism, dominates the gas separation in graphynes. In this context, small gas molecules (e.g., H_2 and He) are expected to permeate through graphdiyne pores freely while large gas molecules (e.g., CH_4) are rejected, in agreement with aforementioned observations. However, other molecular sieving phenomenon such as quantum sieving and chemical affinity sieving may also be effective depending on molecular type, as well as shape, size and edge functionalization of graphyne pores.[32]

4. Challenges to Move Forward

Although a large number of aforementioned theoretical studies have acknowledged the potential of graphynes as one of the most promising alternatives to current state-of-the-art separation membranes, none of the predicted separation process has ever been realized in experiments. In contrast, conventional polymeric membranes are mature and have found applications in many industrial processes. In this regard, the graphyne membranes are still in the early stage of development, and the first following step is to extend the characterization of these membranes beyond theoretical predictions and into experimental validations. The subsequent development of graphyne-based membranes may include at least the following stages: experimental proof-of-principle devices, lab-scale membranes, industrial-scale membranes with acceptable stability and cost-effectiveness, etc. During every stage of the development, it is undoubted that lots of technological challenges have to be overcome. We discuss here the main challenges faced now and in the near future: high-quality fabrication and maintenance of structural robustness of graphynes as well as accurate computational characterization of graphyne separation performance.

4.1. Fabrication of High-Quality Graphyne Membranes

The first and foremost step to the possible success of graphyne-based membranes is the fabrication of high-quality and large-area graphyne materials, first in proof-of-principle experiments in the laboratory and eventually in a scalable and economical way suitable for industry. Particularly, the quality of graphyne is the decisive factor for membrane applications, as the presence of defects such as vacancies, tears and wrinkles would largely suppress the separation performance, especially the selectivity. As the next step toward membrane applications, the transfer of fabricated graphynes to supporting porous substrates is also crucial, during which graphynes have to maintain at least a certain extent of mechanical strength to withstand loading pressures in separation applications.

In the case of graphene preparation, a few-layer and even monolayer sheet could be created directly from bulk graphite by chemical or mechanical exfoliation, a well-known top-down method.[82] However, as no bulk phase is experimentally available for graphynes, it is impossible to synthesize graphyne with this top-down approach. On the other hand, using a bottom-up method instead, one needs to go down to the molecular scale and start from precursor molecules that contain acetylenic linkages. With suitable precursor in hand, we could obtain, in principle, a 2D extended structure by controlled chemical reactions between precursor molecules. However, traditional organic synthesis yielded only graphdiyne substructures (or subunits) with a maximum of four structural units, due to the complex synthetic steps, low production rate and the low solubility.[53,83] A breakthrough in graphyne synthesis was made in 2010 by Li and co-workers, who reported that 2D graphdiyne sheets of 1 μm thick were successfully fabricated via cross-coupling reaction on Cu foil surfaces, using hexaethynylbenzene (HEB) as precursor.[29] The Cu foil therein acts as both the reaction substrate and the source of Cu^{2+} ions to catalyze the cross-coupling reaction. The fabricated graphdiyne films are uniform, consisting of graphdiyne multilayers. Through a chemical vapor deposition (CVD) process with HEB again as the precursor, a linked monolayer carbon network with acetylenic scaffoldings, graphdiyne analogs, could be prepared.[84] However, transmission electron microscopy (TEM) image of the resulting film indicated that the structure shows no significant in-plane order over the tested area. To construct well-ordered molecular structures in large area, such as graphdiyne, rational design of the catalytic environment such as temperature and preprocess to the substrates is necessary for this CVD method.

Recently, Liu, Zhang and coworkers obtained continuous flat ultrathin graphdiyne film with thickness less than 3 nm (6–10 layers) by using graphene as a surface template.[85] They also created graphdiyne-based field-effect transistor (FET) devices after extending this template method to hexagonal boron nitride (*h*BN), and determined lower FET mobility than that theoretically predicted. This observation highlights the need to optimize the template method to minimize defects and maximize domains, in order to improve the quality of graphdiyne. Matsuoka et al. reported the bottom-up synthesis of crystalline graphdiyne nanosheets through a liquid/liquid or gas/liquid interfacial protocol with HEB as the precursor.[86] The resulting single-crystalline graphdiyne nanosheets have regular hexagonal domains with a uniform thickness of 3.0 nm and a lateral size of 1.5 μm. For experimental efforts made into the fabrication of graphdiyne, not limited to those described here, the reader is directed to several excellent reviews.[30,33,53] Despite the enormous progress, the fabrication of a monolayer graphdiyne remains extremely challenging. What's worse, the preparation of other members in graphyne family, particularly those proven suitable for desalination (e.g., graphyne-3, α-graphyne and β-graphyne), remains a challenging task. One possible reason is the complicated synthesis of suitable precursors. Recently, after successfully preparing the precursor molecule, tetraethynylethene (TEE), Li et al. synthesized a β-graphyne-containing thin film with thickness of about 25 nm on copper foil using a modified Glaser–Hay coupling reaction.[87] It is reasonable to expect that future improvement in the preparation of graphyne materials should be benefited from surface engineering of substrates or rational design and synthesis of new precursor used in cross-coupling reactions, as well as development of fundamentally new preparation technologies. A deep microscopic understanding of the reaction process and mechanism involved in the growth of such 2D materials, particularly from a theoretical perspective, should be helpful to guide relevant experimental attempts.

4.2. Structural Robustness of Graphynes against Pressures

Another challenge is the maintenance of high mechanical strength of graphynes to avoid any mechanical failure in the clamping process during the fabrication of membrane modules as well as to withstand high operating pressures in separation processes. Furthermore, the stiffness of graphyne is also of importance because excess tensile deformation might lead to significant pore expansion in graphynes, affecting the separation performance. Fortunately, the graphyne architectures were predicted to be mechanically stable with high strength and

stiffness.[88,89] With the increase of acetylene groups, the Young's modulus deceases, while the fracture strain remains almost constant.[89,90] Zhao et al. compared the mechanical properties of graphdiyne with a few other carbon allotropes and highlighted the dominant role of area density (i.e., number of carbon atoms per unit area) in affecting mechanical properties.[91] Lin and Buehler reported MD-based biaxial mechanical tensile tests on a series of graphyne-n (n = 3–6) membranes and obtained ultimate stress and strain fall between 16.7–32.3 GPa and 1.2–2.7%, respectively, which are much higher than conventional polymer based membranes and comparable to those of carbon nanotubes with ultimate stress of 11–63 GPa.[40] In particular, graphyne-3, an ideal candidate for desalination membranes suggested in most MD studies, was proposed to have the highest mechanical properties among the considered graphynes. Finally, this work assessed the impact of mechanical deformation in graphyne-3 on its desalination performance, and noted a small increase in water permeance, while the salt rejection rate was not affected.[40] The structural stability, both in air and in water, is also crucial for the use of graphynes in membrane applications. In principle, the presence of acetylenic linkages in graphynes would decreases their stability relative to those of graphene and other sp^2-like graphene allotropes.[30] Further studies that specifically investigate this aspect are necessary, especially in the context of membrane separation processes.

Although the above progress indicates that a pristine graphyne is a promising candidate as mechanically robust membrane materials, its mechanical property may be largely reduced in practical applications, as synthesized graphynes (also graphene) usually have defects and adsorbed impurities introduced during fabrication, transfer and integration processes. Meanwhile, the introduction of functionalization to regulate its separation performance may also influence its mechanical properties. In this context, further theoretical and experimental efforts could be devoted to addressing these issues to guide the design of graphyne-based membranes. On the other hand, graphyne could withstand higher loading pressures when it is properly supported by a porous substrate, as is usually the case in current commercial membrane modules. In the case of graphene, Cohen–Tanugi and Grossmana predicted that a porous membrane atop a porous substrate with pores less than 1 μm could withstand a loading pressure of 57 MPa, about 10-fold higher than that in commercial RO desalination.[92] It is worth noting that the strength data of supported graphene may not be identical to those of graphyne because they possess different chemical bonds. Meanwhile, as a single layer graphyne of large-area and high-quality has not been experimentally available, its real mechanical strength is yet to be measured. Nonetheless, reinforcement is expectable in graphyne membranes on supporting porous substrates with appropriate pores. In this regard, future work is needed to optimize the structural design of the porous substrate layer as well as its adhesion to graphynes to produce mechanically robust membrane modules.

4.3. Computational Characterization of Separation Performance

Diversity in the quantitative and even qualitative characterization of permeance and selectivity exists among different theoretical studies, highlighting the need of further comprehensive theoretical investigations. For instance, a MD study argued that graphyne-4 can also achieve complete salt rejection and concurrently a higher water permeance (than graphyne-3),[41] while other studies reported incomplete salt rejection for graphyne-4, especially under high pressures.[39,52,55] Difference in the choice of the water model and strategies for pressure loading may account for such inconsistence; it is necessary to conduct systematical theoretical studies (e.g., with both MD and DFT) to figure out how the predicted performance depends on these parameters. A further concern related to computational approaches is the accurate determination of both permeance and selectivity. On one hand, MD simulations could better determine the permeance based on sufficient number of permeation events of desired species, but have difficulties in determining high selectivity due to the limited permeation events of undesired species. On the other hand, DFT studies could predict extremely high selectivity based on energy landscape but fail to consider the influence of molecule population as well as temperature and pressure fluctuations in practical systems. Although the combination of these existing methods (e.g., QM/MD) offers a possible route to address this issue, novel computational approaches are also desired.

5. Future Outlook

In the aforesaid section, we have shown that there are a number of inherent challenges, particularly on the experimental side, that have to be overcome to push graphynes toward practical separation applications. In addition, other potential future opportunities related to fundamental understanding of graphyne-based separation processes are presented and discussed as follows.

5.1. Possible New Membrane Applications

Aside from technical development toward the experimental realization of the predicted separations, theoretical studies on fundamental principles are still in demand, for example, to search for other applications of graphyne membranes and to improve their separation performance through a deeper understanding of how molecules behave inside graphyne nanopores. In particular, it is known that the molecular sieving mechanism governs the mass transport through neutral graphyne pores, in which larger particles than the pore size can be separated out. In this context, a rational choice of graphyne types, along with appropriate chemical modifications, is helpful to design membranes for other important separation applications such as water pretreatment and production of ultrapure nitrogen or oxygen.

5.2. Assembly of Graphyne Membranes

Another possible direction that may advance graphynes for practical applications is the use of a multilayer membrane rather than the monolayer ones reported in majority of current theoretical literature. Note that the experimentally available graphdiyne is not a monolayer sheet, but rather, a few-layer structure.[29,30] Indeed, not limited to graphyne, the use of a multilayer sheet is

also meaningful for porous graphene as separation membranes, due to its cost efficiency with respect to a monolayer one. It was theoretically predicted that the desalination performance of a multilayer porous graphene could be modulated by adjusting the vertical spacing (so-called pore offset) between two graphene layers and/or the transverse distance between two pores.[93] It is interesting to note that the salt rejection of the multilayer porous graphene could be significantly promoted by increasing the pore offset; the increased salt rejection resulted from additional barriers to ion transport added by the narrow interlayer region.[93] Nevertheless, significant technological challenges remain in introducing an precise offset in pore creation experiments, as nanopores in a multilayer graphene sheet machined by focused ion beams or electron beams tend to form a highly aligned arrangement, namely, without the offset. In this regard, the intrinsic nanopores in graphyne provide fascinating opportunities to fulfill such mission, as no pore fabrication process is needed for graphyne. For instance, the offset could be introduced and controlled in a multilayer structure of graphyne by considering different interlayering stacking.

Recently, a multilayer sheet of graphyne-3 was constructed successfully based on DFT calculations, and the optimal structures are stacked in ABA-like configurations with an average interlayer spacing of ≈3.45 Å.[94] The lateral pore offset (i.e., displacement of one layer with respect with its adjacent ones) is only ≈1.6 Å. The nanochannels formed by spatial connection between pores on different sheets are permeable to light gas species such as CO_2, N_2, H_2O, and H_2.[94] Very recently, an MD study by Akhavan et al. reported the desalination performance of graphyne-3 and graphyne-4 in a double-layer configuration, either AA- or AB-stacking, and noted an increase in salt rejection of the double-layer graphene-4 compared to the single-layer one.[95] As the interlayer spacing varies, the highest water permeability was seen at a spacing of ≈3.5 Å, and nearly vanished at a spacing of ≈6 Å. Furthermore, the difference in water permeability between AA- and AB-stacked graphyne-3 is evident at smaller spacing but becomes insignificant at larger spacing.[95] Further extensive studies are required to optimize the separation performance by altering the number of graphyne layers, the stacking configurations, graphyne types, etc.

5.3. Graphyne-Like Nanoporous Membranes

Another 2D carbon nanomaterial that may revolutionize membrane technologies is porous graphene, which is structurally analogous to graphynes; they are both stronger and thinner than the polyamide selective layers in TFC membranes. Resembling graphynes, intrinsic defects acting as nanopores can be formed during the growth and transfer processes of graphene.[96] Other approaches such as ion and electron beams as well as oxygen plasma etching process, were also widely used in the pore creation in graphene membranes.[9] The shape and size of graphene pores usually fall in a wide range (i.e., lack of uniformity), thus hampering its selectivity. Narrowing the pore size distribution is therefore an important task in graphene membranes. In the case of graphyne, the pore uniformity can be readily achieved if the fabricated samples are in large area and high quality. However, as discussed earlier, the controlled fabrication of graphyne is extremely challenging. On the

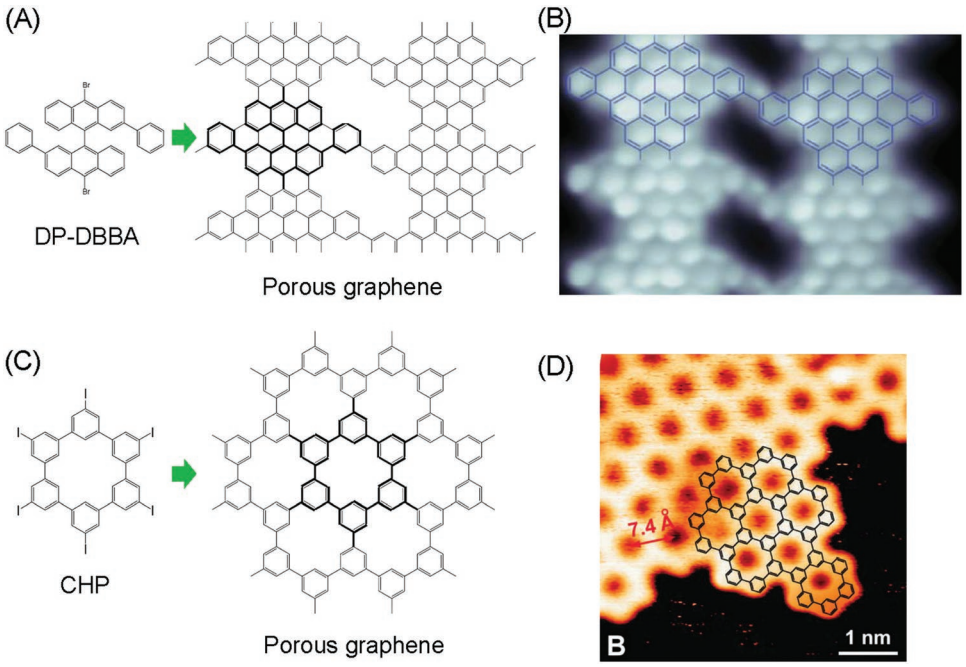

Figure 8. The emergence of graphyne-like atomically thin membrane. A) Porous graphene containing nanopores with a uniform diameter of ≈1 nm fabricated through a bottom-up method using the molecular precursor DP-DPPA. B) STM image showing the structure of the porous graphene. A,B) Reproduced with permission.[97] Copyright 2018, American Association for the Advancement of Science. (C) and (D) are identical to (A) and (B) but using the molecular precursor CHP and therefore correspond to a different porous graphene. C,D) Reproduced with permission.[99] Copyright 2009, Royal Society of Chemistry.

other hand, all the graphyne-based separation processes were reported by theoretical studies; a proof-of-concept experimental device for graphyne-based separation has not been reported yet. In this regard, the development of porous graphene membranes, from an engineering standpoint, is far beyond that of graphyne. This is because a large number of studies, either theoretically or experimentally, have been carried out to explore various aspects of porous graphene relating to separation applications, including material fabrication, pore creation, defect sealing and large-scale integration, *etc*. Interested readers are directed to a comprehensive review summarizing the potential of graphene membranes for water desalination.[9]

Porous graphene may become structurally more like graphyne if a controlled bottom-up synthesis method, similar to those used in graphyne synthesis, could be available in the preparation of porous graphene. Actually, this bottom-up method has proved itself quite useful in the fabrication of porous graphene containing uniform pores, a feature seemingly exclusive to graphyne. Very recently, Moreno et al. reported the bottom-up synthesis of nanoporous graphene containing an ordered array of ≈1 nm diameter nanopores.[97] The monomer precursor used in this work is diphenyl-10,10′-dibromo-9,9′-bianthracene (DP-DBBA). After a few steps of deposition and annealing to different temperatures on an Au (111) surface, the monomer underwent the transition to intermediate structures including polymers and graphene nanoribbons. The final product is a porous graphene sheet (**Figure 8**A,B) that features a uniform distribution in pore shape and size, just like graphynes.[97,98] In addition, the use of another molecular precursor, hexaiodo-substituted macrocycle cyclohexa-*m*-phenylene (CHP), yielded a completely different pore structure, also uniform in size and shape (Figure 8C,D). This structure corresponds to another type of porous graphene,[99] which has been predicted to exhibit an extremely high selectivity ratio for H_2 and He over other gases such as Ne, O_2, N_2, and CO_2.[100] Despite much progress, further intensive efforts relating to the bottom-up synthesis of these graphyne-like nanomaterials are still in demand, for example, concentrating on improving scalability and quality of fabrication and developing appropriate molecular precursor for desired pore dimensions.

6. Conclusions

A number of investigations, mostly from a theoretical viewpoint, have demonstrated the remarkable performance of graphynes in applications of water desalination and gas separation. In particular, the theoretically predicted water permeance of certain graphynes like graphyne-3 is about two orders of magnitude higher than the experimental values for current state-of-the-art RO membranes while at the same time maintaining nearly 100% salt rejection. The separation performance could be further promoted by engineering of the pore edges and membrane's surfaces. Since graphyne-based membranes are still in the early stage of development, there are a number of challenges that have to be overcome, in order to transfer the theoretical predictions to lab-scale experimental devices, and finally to practical applications at the industrial scale. These challenges include chemical fabrication of various graphynes in large area and high quality, integration techniques into membrane modules, as well as fundamental understanding of the transport process and how it depends on the pore shape, pore size and the interlayer stacking in the case of multilayer graphynes. However, the intriguing advantages associated with its unique pore characteristics of graphyne should be able to inspire researchers to continue their efforts. On the other hand, an encouraging opportunity arises due to the successful bottom-up synthesis of nanoporous graphene containing uniform pores, highlighting the possibility to utilize graphyne-like membrane materials, not limited to graphyne itself, in separation technologies.

Acknowledgements

This article is part of a special section on graphdiyne. This work was supported by the National Natural Science Foundation of China (11772152, 51535005, 11772153, and 51472117), the Jiangsu Province NSF (BK20180065), the Research Fund of State Key Laboratory of Mechanics and Control of Mechanical Structures (MCMS-0417G03, MCMS-I-0418K01), the Fundamental Research Funds for the Central Universities (NP2017101, NC2018001, NE2018002), and a project funded by the Priority Academic Program Development of Jiangsu Higher Education Institutions.

Conflict of Interest

The authors declare no conflict of interest.

Keywords

2D materials, gas separation, graphdiyne, graphyne, membranes, reverse osmosis

Received: June 14, 2018
Revised: October 31, 2018
Published online: January 28, 2019

[1] S. S. Shenvi, A. M. Isloor, A. F. Ismail, *Desalination* **2015**, *368*, 10.
[2] L. F. Greenlee, D. F. Lawler, B. D. Freeman, B. Marrot, P. Moulin, *Water Res.* **2009**, *43*, 2317.
[3] K. P. Lee, T. C. Arnot, D. Mattia, *J. Membr. Sci.* **2011**, *370*, 1.
[4] S.-Y. Kwak, D. Woo Ihm, *J. Membr. Sci.* **1999**, *158*, 143.
[5] A. G. Fane, R. Wang, M. X. Hu, *Angew. Chem., Int. Ed.* **2015**, *54*, 3368.
[6] T. Uragami, *Science and Technology of Separation Membranes*, John Wiley & Sons, Hoboken, NJ, USA **2017**.
[7] P. Pandey, R. S. Chauhan, *Prog. Polym. Sci.* **2001**, *26*, 853.
[8] D. Cohen-Tanugi, J. C. Grossman, *Desalination* **2015**, *366*, 59.
[9] S. Homaeigohar, M. Elbahri, *NPG Asia Mater.* **2017**, *9*, e427.
[10] L. Wang, M. S. H. Boutilier, P. R. Kidambi, D. Jang, N. G. Hadjiconstantinou, R. Karnik, *Nat. Nanotechnol.* **2017**, *12*, 509.
[11] M. R. Chowdhury, J. Steffes, B. D. Huey, J. R. McCutcheon, *Science* **2018**, *361*, 682.
[12] S. Kar, R. C. Bindal, P. K. Tewari, *Nano Today* **2012**, *7*, 385.
[13] a) B. Zhu, D. T. Myat, J.-W. Shin, Y.-H. Na, I.-S. Moon, G. Connor, S. Maeda, G. Morris, S. Gray, M. Duke, *J. Membr. Sci.* **2015**, *475*, 167; b) L. Li, J. Dong, T. M. Nenoff, R. Lee, *J. Membr. Sci.* **2004**, *243*, 401.
[14] J. K. Holt, H. G. Park, Y. Wang, M. Stadermann, A. B. Artyukhin, C. P. Grigoropoulos, A. Noy, O. Bakajin, *Science* **2006**, *312*, 1034.

[15] F. Fornasiero, H. G. Park, J. K. Holt, M. Stadermann, C. P. Grigoropoulos, A. Noy, O. Bakajin, *Proc. Natl. Acad. Sci. USA* **2008**, *105*, 17250.
[16] B. Corry, *J. Phys. Chem. B* **2008**, *112*, 1427.
[17] M. S. Mauter, M. Elimelech, *Environ. Sci. Technol.* **2008**, *42*, 5843.
[18] a) R. K. Joshi, P. Carbone, F. C. Wang, V. G. Kravets, Y. Su, I. V. Grigorieva, H. A. Wu, A. K. Geim, R. R. Nair, *Science* **2014**, *343*, 752; b) B. Mi, *Science* **2014**, *343*, 740; c) K. G. Zhou, K. S. Vasu, C. T. Cherian, M. Neek-Amal, J. C. Zhang, H. Ghorbanfekr-Kalashami, K. Huang, O. P. Marshall, V. G. Kravets, J. Abraham, Y. Su, A. N. Grigorenko, A. Pratt, A. K. Geim, F. M. Peeters, K. S. Novoselov, R. R. Nair, *Nature* **2018**, *559*, 236; d) S. Homaeigohar, T. Strunskus, J. Strobel, L. Kienle, M. Elbahri, *Adv. Mater. Interfaces* **2018**, *5*, 1800001.
[19] H. M. Hegab, L. Zou, *J. Membr. Sci.* **2015**, *484*, 95.
[20] Y. You, V. Sahajwalla, M. Yoshimura, R. K. Joshi, *Nanoscale* **2016**, *8*, 117.
[21] G.-R. Xu, J.-M. Xu, H.-C. Su, X.-Y. Liu, L. Lu, H.-L. Zhao, H.-J. Feng, R. Das, *Desalination* **2019**, *451*, 18.
[22] A. K. Geim, *Science* **2009**, *324*, 1530.
[23] a) D. Cohen-Tanugi, J. C. Grossman, *Nano Lett.* **2012**, *12*, 3602; b) M. E. Suk, N. R. Aluru, *J. Phys. Chem. Lett.* **2010**, *1*, 1590; c) K. Sint, B. Wang, P. Král, *J. Am. Chem. Soc.* **2008**, *130*, 16448.
[24] D. Konatham, J. Yu, T. A. Ho, A. Striolo, *Langmuir* **2013**, *29*, 11884.
[25] S. P. Surwade, S. N. Smirnov, I. V. Vlassiouk, R. R. Unocic, G. M. Veith, S. Dai, S. M. Mahurin, *Nat. Nanotechnol.* **2015**, *10*, 459.
[26] W. Li, Y. Yang, J. K. Weber, G. Zhang, R. Zhou, *ACS Nano* **2016**, *10*, 1829.
[27] M. Heiranian, A. B. Farimani, N. R. Aluru, *Nat. Commun.* **2015**, *6*, 8616.
[28] a) Q. Xu, H. Xu, J. Chen, Y. Lv, C. Dong, T. S. Sreeprasad, *Inorg. Chem. Front.* **2015**, *2*, 417; b) A. A. Ramanathan, M. W. Aqra, A. E. Al-Rawajfeh, *Environ. Chem. Lett.* **2018**, *16*, 1217.
[29] G. Li, Y. Li, H. Liu, Y. Guo, Y. Li, D. Zhu, *Chem. Commun.* **2010**, *46*, 3256.
[30] Y. Li, L. Xu, H. Liu, Y. Li, *Chem. Soc. Rev.* **2014**, *43*, 2572.
[31] a) P. S. Goh, A. F. Ismail, *Desalination* **2015**, *356*, 115; b) T. Humplik, J. Lee, S. C. O'Hern, B. A. Fellman, M. A. Baig, S. F. Hassan, M. A. Atieh, F. Rahman, T. Laoui, R. Karnik, E. N. Wang, *Nanotechnology* **2011**, *22*, 292001; c) A. Aghigh, V. Alizadeh, H. Y. Wong, M. S. Islam, N. Amin, M. Zaman, *Desalination* **2015**, *365*, 389.
[32] Y. Jiao, A. Du, M. Hankel, S. C. Smith, *Phys. Chem. Chem. Phys.* **2013**, *15*, 4832.
[33] a) A. L. Ivanovskii, *Prog. Solid State Chem.* **2013**, *41*, 1; b) Z. Chen, C. Molina-Jirón, S. Klyatskaya, F. Klappenberger, M. Ruben, *Ann. Phys.* **2017**, *529*, 1700056; c) J. Z. Jingyuan Zhou, Zhongfan Liu, *Acta Phys.-Chim. Sin.* **2018**, *34*, 977; d) Y. L. Yongjun Li, *Acta Phys.-Chim. Sin.* **2018**, *34*, 992.
[34] a) Q. Peng, A. K. Dearden, J. Crean, L. Han, S. Liu, X. Wen, S. De, *Nanotechnol., Sci. Appl.* **2014**, *7*, 1; b) H. Tang, C. M. Hessel, J. Wang, N. Yang, R. Yu, H. Zhao, D. Wang, *Chem. Soc. Rev.* **2014**, *43*, 4281; c) J. Xi, D. Wang, Z. Shuai, *Wiley Interdiscip. Rev.: Comput. Mol. Sci.* **2015**, *5*, 215; d) F. Chang, *Int. J. Electrochem. Sci.* **2017**, 10348; e) C. Ge, J. Chen, S. Tang, Y. Du, N. Tang, *ACS Appl. Mater. Interfaces* **2018**, https://doi.org/10.1021/acsami.8b03413; f) J. Kang, Z. Wei, J. Li, *ACS Appl. Mater. Interfaces* **2018**, https://doi.org/10.1021/acsami.8b03338.
[35] A. Hirsch, *Nat. Mater.* **2010**, *9*, 868.
[36] H. W. Kroto, J. R. Heath, S. C. O'Brien, R. F. Curl, R. E. Smalley, *Nature* **1985**, *318*, 162.
[37] S. Iijima, *Nature* **1991**, *354*, 56.
[38] K. S. Novoselov, A. K. Geim, S. V. Morozov, D. Jiang, Y. Zhang, S. V. Dubonos, I. V. Grigorieva, A. A. Firsov, *Science* **2004**, *306*, 666.
[39] M. Xue, H. Qiu, W. Guo, *Nanotechnology* **2013**, *24*, 505720.
[40] S. Lin, M. J. Buehler, *Nanoscale* **2013**, *5*, 11801.
[41] C. Zhu, H. Li, X. C. Zeng, E. G. Wang, S. Meng, *Sci. Rep.* **2013**, *3*, 3163.
[42] Y. Jiao, A. Du, M. Hankel, Z. Zhu, V. Rudolph, S. C. Smith, *Chem. Commun.* **2011**, *47*, 11843.
[43] S. W. Cranford, M. J. Buehler, *Nanoscale* **2012**, *4*, 4587.
[44] Y. Pan, Y. Wang, L. Wang, H. Zhong, R. Quhe, Z. Ni, M. Ye, W. N. Mei, J. Shi, W. Guo, J. Yang, J. Lu, *Nanoscale* **2015**, *7*, 2116.
[45] G. Li, Y. Li, X. Qian, H. Liu, H. Lin, N. Chen, Y. Li, *J. Phys. Chem. C* **2011**, *115*, 2611.
[46] a) S. Zhang, H. Du, J. He, C. Huang, H. Liu, G. Cui, Y. Li, *ACS Appl. Mater. Interfaces* **2016**, *8*, 8467; b) S. Zhang, H. Liu, C. Huang, G. Cui, Y. Li, *Chem. Commun.* **2015**, *51*, 1834; c) K. Wang, N. Wang, J. He, Z. Yang, X. Shen, C. Huang, *ACS Appl. Mater. Interfaces* **2017**, *9*, 40604; d) C. Huang, S. Zhang, H. Liu, Y. Li, G. Cui, Y. Li, *Nano Energy* **2015**, *11*, 481.
[47] a) S. Wang, L. Yi, J. E. Halpert, X. Lai, Y. Liu, H. Cao, R. Yu, D. Wang, Y. Li, *Small* **2012**, *8*, 265; b) J. Li, X. Gao, B. Liu, Q. Feng, X. B. Li, M. Y. Huang, Z. Liu, J. Zhang, C. H. Tung, L. Z. Wu, *J. Am. Chem. Soc.* **2016**, *138*, 3954.
[48] a) X. Chen, P. Gao, L. Guo, S. Zhang, *Sci. Rep.* **2015**, *5*, 16720; b) N. Parvin, Q. Jin, Y. Wei, R. Yu, B. Zheng, L. Huang, Y. Zhang, L. Wang, H. Zhang, M. Gao, H. Zhao, W. Hu, Y. Li, D. Wang, *Adv. Mater.* **2017**, *29*, 1606755.
[49] J. S. Bunch, S. S. Verbridge, J. S. Alden, A. M. van der Zande, J. M. Parpia, H. G. Craighead, P. L. McEuen, *Nano Lett.* **2008**, *8*, 2458.
[50] a) Q. Yuan, Y.-P. Zhao, *Phys. Rev. Lett.* **2010**, *104*, 246101; b) H. Qiu, R. Shen, W. Guo, *Nano Res.* **2011**, *4*, 284; c) H. Qiu, W. Guo, *Phys. Rev. Lett.* **2013**, *110*, 195701; d) J. Zhao, L. Kou, J. W. Jiang, T. Rabczuk, *Nanotechnology* **2014**, *25*, 295701; e) N. Wei, C. Lv, Z. Xu, *Langmuir* **2014**, *30*, 3572; f) H. Qiu, X. C. Zeng, W. Guo, *ACS Nano* **2015**, *9*, 9877; g) Z. Yang, J. Zhao, N. Wei, *Appl. Phys. Lett.* **2015**, *107*, 023107; h) Y. Zhu, F. Wang, J. Bai, X. C. Zeng, H. Wu, *ACS Nano* **2015**, *9*, 12197; i) H. Qiu, M. Xue, C. Shen, W. Guo, *Nanoscale* **2018**, *10*, 8962.
[51] J. Kou, X. Zhou, Y. Chen, H. Lu, F. Wu, J. Fan, *J. Chem. Phys.* **2013**, *139*, 064705.
[52] J. Kou, X. Zhou, H. Lu, F. Wu, J. Fan, *Nanoscale* **2014**, *6*, 1865.
[53] C. Huang, Y. Li, N. Wang, Y. Xue, Z. Zuo, H. Liu, Y. Li, *Chem. Rev.* **2018**, *118*, 7744.
[54] B. Wu, H. Jin, J. Yin, W. Zhang, X. Tang, P. Zhang, Y. Ding, *Carbon* **2017**, *123*, 688.
[55] M. Raju, P. B. Govindaraju, A. C. T. van Duin, M. Ihme, *Nanoscale* **2018**, *10*, 3969.
[56] X. Zhang, J.-G. Gai, *RSC Adv.* **2015**, *5*, 68109.
[57] M. Bartolomei, E. Carmona-Novillo, M. I. Hernandez, J. Campos-Martinez, F. Pirani, G. Giorgi, K. Yamashita, *J. Phys. Chem. Lett.* **2014**, *5*, 751.
[58] F. Liu, J. Yang, Z. Xu, X. Yang, *Appl. Surf. Sci.* **2016**, *387*, 1080.
[59] J. Yang, Z. Xu, X. Yang, *Phys. Chem. Chem. Phys.* **2017**, *19*, 21481.
[60] W. Zhang, Z. Xu, X. Yang, *Chin. J. Chem. Eng.* **2018**, https://doi.org/10.1016/j.cjche.2018.02.028.
[61] J. R. Werber, A. Deshmukh, M. Elimelech, *Environ. Sci. Technol. Lett.* **2016**, *3*, 112.
[62] D. Cohen-Tanugi, R. K. McGovern, S. H. Dave, J. H. Lienhard, J. C. Grossman, *Energy Environ. Sci.* **2014**, *7*, 1134.
[63] S. Zhao, J. Xue, W. Kang, *J. Chem. Phys.* **2013**, *139*, 114702.
[64] D. E. Jiang, V. R. Cooper, S. Dai, *Nano Lett.* **2009**, *9*, 4019.
[65] J. Schrier, *J. Phys. Chem. Lett.* **2010**, *1*, 2284.
[66] H. Du, J. Li, J. Zhang, G. Su, X. Li, Y. Zhao, *J. Phys. Chem. C* **2011**, *115*, 23261.
[67] A. Ambrosetti, P. L. Silvestrelli, *J. Phys. Chem. C* **2014**, *118*, 19172.
[68] S. P. Koenig, L. Wang, J. Pellegrino, J. S. Bunch, *Nat. Nanotechnol.* **2012**, *7*, 728.

[69] K. Celebi, J. Buchheim, R. M. Wyss, A. Droudian, P. Gasser, I. Shorubalko, J. I. Kye, C. Lee, H. G. Park, *Science* **2014**, *344*, 289.
[70] H. Zhang, X. He, M. Zhao, M. Zhang, L. Zhao, X. Feng, Y. Luo, *J. Phys. Chem. C* **2012**, *116*, 16634.
[71] W.-h. Zhao, L.-f. Yuan, J.-l. Yang, *Chin. J. Chem. Phys.* **2012**, *25*, 434.
[72] M. Bartolomei, E. Carmona-Novillo, M. I. Hernández, J. Campos-Martínez, F. Pirani, G. Giorgi, *J. Phys. Chem. C* **2014**, *118*, 29966.
[73] Y. B. Apriliyanto, N. Faginas Lago, A. Lombardi, S. Evangelisti, M. Bartolomei, T. Leininger, F. Pirani, *J. Phys. Chem. C* **2018**, *122*, 16195.
[74] Z. Meng, X. Zhang, Y. Zhang, H. Gao, Y. Wang, Q. Shi, D. Rao, Y. Liu, K. Deng, R. Lu, *ACS Appl. Mater. Interfaces* **2016**, *8*, 28166.
[75] Y. Jiao, A. Du, S. C. Smith, Z. Zhu, S. Z. Qiao, *J. Mater. Chem. A* **2015**, *3*, 6767.
[76] J. Xu, J. Li, H. J. Liu, L. M. Zhao, *Defect Diffusion Forum* **2017**, *381*, 20.
[77] X. Tan, L. Kou, H. A. Tahini, S. C. Smith, *Mol. Simul.* **2016**, *42*, 573.
[78] M. Alaghemandi, *Chem. Phys. Lett.* **2015**, *629*, 65.
[79] P. Sang, L. Zhao, J. Xu, Z. Shi, S. Guo, Y. Yu, H. Zhu, Z. Yan, W. Guo, *Int. J. Hydrogen Energy* **2017**, *42*, 5168.
[80] L. Zhao, P. Sang, S. Guo, X. Liu, J. Li, H. Zhu, W. Guo, *Appl. Surf. Sci.* **2017**, *405*, 455.
[81] J. M. Bielza, H. Kamusewitz, M. Keller, D. Paul, *Langmuir* **2002**, *18*, 8129.
[82] J. A. Rogers, M. G. Lagally, R. G. Nuzzo, *Nature* **2011**, *477*, 45.
[83] M. M. Haley, S. C. Brand, J. J. Pak, *Angew. Chem. Int., Ed. Engl.* **1997**, *36*, 836.
[84] R. Liu, X. Gao, J. Zhou, H. Xu, Z. Li, S. Zhang, Z. Xie, J. Zhang, Z. Liu, *Adv. Mater.* **2017**, *29*, 1604665.
[85] J. Zhou, Z. Xie, R. Liu, X. Gao, J. Li, Y. Xiong, L. Tong, J. Zhang, Z. Liu, *ACS Appl. Mater. Interfaces* **2018**, https://doi.org/10.1021/acsami.8b02612.
[86] R. Matsuoka, R. Sakamoto, K. Hoshiko, S. Sasaki, H. Masunaga, K. Nagashio, H. Nishihara, *J. Am. Chem. Soc.* **2017**, *139*, 3145.
[87] J. Li, Z. Xie, Y. Xiong, Z. Li, Q. Huang, S. Zhang, J. Zhou, R. Liu, X. Gao, C. Chen, L. Tong, J. Zhang, Z. Liu, *Adv. Mater.* **2017**, *29*, 1700421.
[88] Y. Y. Zhang, Q. X. Pei, C. M. Wang, *Appl. Phys. Lett.* **2012**, *101*, 081909.
[89] Y. Yang, X. Xu, *Comput. Mater. Sci.* **2012**, *61*, 83.
[90] S. W. Cranford, D. B. Brommer, M. J. Buehler, *Nanoscale* **2012**, *4*, 7797.
[91] J. Zhao, N. Wei, Z. Fan, J. W. Jiang, T. Rabczuk, *Nanotechnology* **2013**, *24*, 095702.
[92] D. Cohen-Tanugi, J. C. Grossman, *Nano Lett.* **2014**, *14*, 6171.
[93] D. Cohen-Tanugi, L. C. Lin, J. C. Grossman, *Nano Lett.* **2016**, *16*, 1027.
[94] M. Bartolomei, G. Giorgi, *ACS Appl. Mater. Interfaces* **2016**, *8*, 27996.
[95] M. Akhavan, J. Schofield, S. Jalili, *Phys. Chem. Chem. Phys.* **2018**, *20*, 13607.
[96] S. C. O'Hern, C. A. Stewart, M. S. Boutilier, J. C. Idrobo, S. Bhaviripudi, S. K. Das, J. Kong, T. Laoui, M. Atieh, R. Karnik, *ACS Nano* **2012**, *6*, 10130.
[97] C. Moreno, M. Vilas-Varela, B. Kretz, A. Garcia-Lekue, M. V. Costache, M. Paradinas, M. Panighel, G. Ceballos, S. O. Valenzuela, D. Pena, A. Mugarza, *Science* **2018**, *360*, 199.
[98] A. Sinitskii, *Science* **2018**, *360*, 154.
[99] M. Bieri, M. Treier, J. Cai, K. Ait-Mansour, P. Ruffieux, O. Groning, P. Groning, M. Kastler, R. Rieger, X. Feng, K. Mullen, R. Fasel, *Chem. Commun.* **2009**, 6919.
[100] S. Blankenburg, M. Bieri, R. Fasel, K. Mullen, C. A. Pignedoli, D. Passerone, *Small* **2010**, *6*, 2266.